Plant Methods

RESEARCH

Open Access

Local mapping of root orientation traits by X-ray micro-CT and 3d image analysis: A study case on carrot seedlings grown in simulated vs real weightlessness

L. Gargiulo[1], G. Mele[1*], L. G. Izzo[2], L. E. Romano[2] and G. Aronne[2]

Abstract

Background Root phenotyping is particularly challenging because of complexity and inaccessibility of root apparatus. Orientation is one of the most important architectural traits of roots and its characterization is generally addressed using multiple approaches often based on overall measurements which are difficult to correlate to plant specific physiological aspects and its genetic features. Hence, a 3D image analysis approach, based on the recent method of Straumit, is proposed in this study to obtain a local mapping of root angles.

Results Proposed method was applied here on radicles of carrot seedlings grown in real weightlessness on the International Space Station (ISS) and on Earth simulated weightlessness by clinorotation. A reference experiment in 1 g static condition on Earth was also performed. Radicles were imaged by X-ray micro-CT and two novel root orientation traits were defined: the "root angle to sowing plane" (RASP) providing accurate angle distributions for each analysed radicle and the "root orientation changes" (ROC) number. The parameters of the RASP distributions and the ROC values did not exhibit any significant difference in orientation between radicles grown under clinorotation and on the ISS. Only a slight thickening in root corners was found in simulated vs real weightlessness. Such results showed that a simple uniaxial clinostat can be an affordable analog in experimental studies reckoning on weightless radicles growth.

Conclusions The proposed local orientation mapping approach can be extended also to different root systems providing a contribution in the challenging task of phenotyping complex and important plant structures such as roots.

Keywords X-ray micro-CT, Root phenotyping, Root morphology, Astrobotany, Carrot seedling, Gravitropism

Background

Numerous studies on plant growth in weightless conditions have been conducted since the beginning of the 80's of the last century for their great importance in both the dissection of physiological aspects of plant development on Earth and the perspective of designing future Bioregenerative Life Support Systems (BLSS) in Space (e.g., [3–7, 20, 23, 30]). In addition to cellular and molecular aspects, many studies on the effects of weightlessness are increasingly focusing on plant morphology and in particular on plant root architecture (e.g. [1, 17, 37, 38]).

*Correspondence:
G. Mele
giacomo.mele@cnr.it
[1] Institute for Agricultural and Forest Systems in the Mediterranean, National Research Council, Portici, Italy
[2] Department of Agricultural Sciences, University of Naples Federico II, Portici, Italy

Roots are plant structures specialised to function for anchorage, storage of photo-assimilates, absorption and conduction of water and minerals from soil, which make them very important for gravity response and plant physiology. The root architectural traits are important for the selection of cultivars for crops on Earth and BLSSs with plants aiming, e.g., at the most efficient acquisition of nutrients in such water-limited environments [26] and in general for plant phenotyping to enhance breeding processes [28]. In particular, the root angle is an important drought-adaptive trait that directs the horizontal and vertical distribution of roots into the soil. A strong relation between steep root angle and deep rooting has been observed for example in different cereals, such as wheat [41], rice [18] and sorghum [33]. Root angle is considered overall a basic trait which may explain most of the important phenotypic variation among genotypes [28].

2D image analysis has been by far the most popular approach for quantifying root system architecture, both in seedlings grown on media plates and root crowns excavated from the field [32]. In particular, two-dimensional image analysis has been used also to study the impact of altered gravity conditions on root morphology and thus on root orientation. Since 1994, the root curvature was determined to study the effects of simulated weightless conditions on maize seedling roots, although this was performed manually on enlarged photos [15]. Recently, 2D image analysis was used by Izzo et al. [17] to study the combined effects of several gravity treatments with those of different light wavelengths on root growth orientation of Brassica oleracea seedlings, with the aim of obtaining a thorough knowledge on photomorphogenic and phototropic responses of candidate crops such as B. Oleracea for plant cultivation in altered gravity. In this framework, Villacampa et al. [37] observed that the light avoidance mechanism existing in roots guides their growth orientation towards diminishing light and helps establish the proper longitudinal seedling axis in simulated weightless conditions. 2D image analysis was used also to study the effects of different clinorotation settings on root morphology, and in particular on root curvature, in Arabidopsis thaliana [38] and in 10 different nutritional and economic crops [26].

However, 2D-based measurements have a limitation in that images are typically taken from only one or two camera perspectives and do not represent true root system architecture in its natural form, and thus may omit important information like the root growth angle which is susceptible to measurement errors when 2D projection methods are used [28]. Actually, stereological procedures to overcome such limitations have been proposed such as that based on the method of "total vertical projections" by Wulfsohn et al. [40] and Wulfsohn and Nyengaard [39] to non-destructively estimate total root length, number of branches, diameter distribution and mean root diameter of crested wheatgrass plants (*Agropyron cristatum* L.) growing in a transparent medium.

However, Shao et al. [32] suggest that real 3D imaging and the root architectural traits derived from it have higher heritability, and therefore may be more informative, than methods using 2D imaging. In this regard, the recent technological innovations in scan resolution and the throughput in image processing made X-ray computed tomography (CT) the current state of art technology for non-destructive root phenotyping in soil [13]. Nevertheless, to our knowledge, such technique has never been used in weightless plant growth studies, except for Izzo et al. [16]. Examples of root architecture and in particular root orientation characterization based on micro-CT imaging already exist with different purposes. Flavel et al. [9] non-destructively observed and quantified wheat roots in a repacked Oxisol, in 3D, with and without a band of P-enriched soil. Tracy et al. [36] measured the effect of soil compaction on selected root traits including elongation rate and lateral root angle. Hargreaves et al. [11] compared the architecture of the root system between barley cultivars as measured by 2D scanning of roots grown in a gel chamber, a 3D destructive method using soil, and 3D X-ray micro tomography applied on soil pots.

Different approaches have also been applied for the quantification of the root growth orientation trait based on the type of analysed root systems. For example, Flavel et al. [9] measured the angles of each branch root respect to the axis of the parent root identifying manually one point on each branch root, corresponding to its centroid, as vertex of angle. Tracy et al. [36] measured the root angle respect to the vertical axis identifying manually the ends of each lateral root. Teramoto et al. [35] vectorised a fibrous root system and used the Euclidean coordinates of the ends of each single root in order to calculate the angle between the horizontal line and the root. Schmitz et al. [31] manually traced the adventitious roots emerging from the stem and measured overall their angle respect to a horizontal axis. Gerth et al. [10] instead used the top faces of the calculated convex hull containing the whole root system to define the minimum and maximum angles between the faces and the soil plane.

Summarising, to date there is no standard method for root systems orientation characterization and no method which measures locally the root orientation. Different approaches have been used depending on the type of root system and the aims of the study. In particular, there are no 3D image analysis methods till now proposed to characterise in very detail the direction

changes of roots, as required for plant growing experiments in weightless conditions.

Therefore, in this study we used X-ray micro-CT for imaging of roots aiming at testing a recent 3D image analysis approach based on structure tensor concept for measuring root orientation locally. The research goal was to compare the root growth of carrot seedlings under three different gravitational regimens: static 1g and simulated weightless conditions on Earth, and real weightlessness onboard the International Space Station (ISS).

Methods

Experimental and technical design

Root growth experiment

The carrot radicles analysed in this work were some of those grown in the culture chambers (see Fig. 1g) used in an experiment performed onboard the International Space Station (ISS) on December 2017 during the Expedition 52/53, funded and coordinated by the Italian Space Agency (ASI), along with those grown in the relative Ground Reference Experiment (GRE) in static condition [16]. Carrot seeds resulted the best to fulfil technical requirements of the refurbished hardware BIOKON and

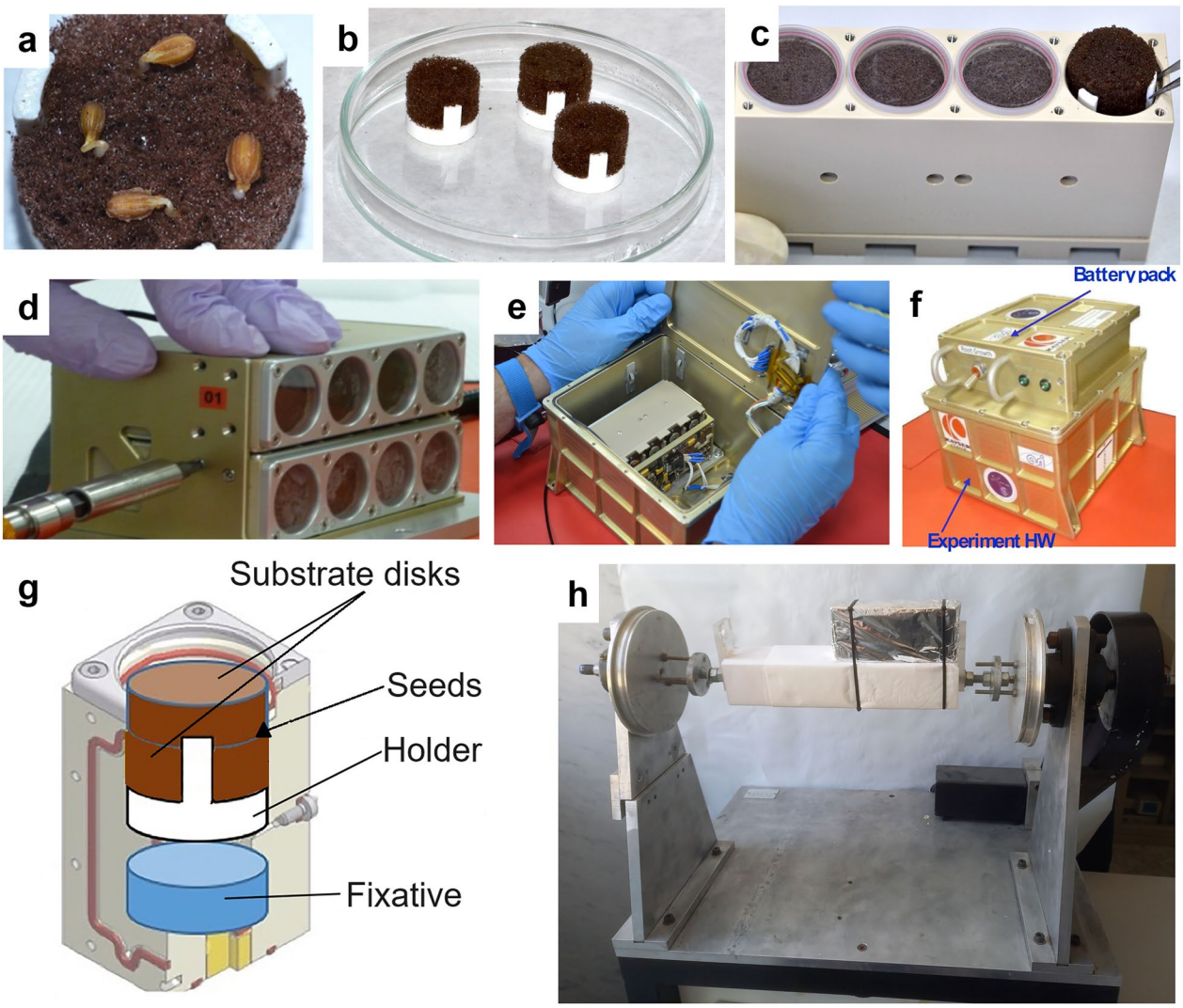

Fig. 1 Hardware equipment used in the experiment. **a** Four carrot seeds positioned on one of the OASIS® substrate disks. **b** OASIS® substrate disks placed on the 3D-printed substrate holders. **c** YING-B2 hardware showing the four culture chambers with OASIS® disks and 3D-printed subtrate holders. **d** Interface plate for accommodating the two YING-B2 units inside the BIOKON. **e** Internal view of the BIOKON with two YING-B2 units. **f** BIOKON container. **g** Schematic of a culture chamber equipped with a fixative reservoir, two substrate disks with seeds, and the 3D-printed substrate holder. **h** Uniaxial clinostat with the YING-B2 unit wrapped in aluminium foil to avoid light interference on root tropisms

YING-B2 (Fig. 1c and f) assigned for the space experiment after tests described in Aronne et al. [2]. From the overall evaluation of the data obtained, the seeds of *D. carota* cv. Chantenay were chosen.

Four carrot seeds were placed in each culture chamber between two equal cylinders of substrate Oasis Grower Foam (Oasis® Growing Solutions, The Netherlands), a phenolic plastic foam, commonly used for soilless cultivations, tightened by a 3D-printed holder (see Fig. 1b). Such substrate assemblage and its holder are named in the following as SH. After 175 *h* from seed sowing, the radicle development onboard the ISS was stopped by activating the injection of a fixative solution, therefore concluding the experiment in real weightless conditions. RNALater (Sigma-Aldrich, St. Louis, Missouri, US) was used as chemical fixative. After the flight experiment, the GRE on Earth was performed using the same hardware, the same batch of seeds, and the same duration and environmental conditions recorded during the experiment on the ISS as more exhaustively described in Izzo et al. [16].

In addition, in the current study also radicles grown on a uniaxial clinostat (CL) were considered in order to perform an experiment which simulates weightless conditions on Earth [12, 21]. The same culture chambers and SH used for the ISS and GRE experiments were used in CL (Fig. 1h). Two rotations/minute of clinostat and seeds distance from rotation axis of about 2 cm induced the negligible centrifugal acceleration respect to gravitation of about 8.94×10^{-5} *g*. CL experiment was also performed with the same duration of the flight experiment and using the same temperature regime recorded during the spaceflight.

3d imaging and analysis

A scheme of root image acquisition, processing and analysis is reported in Fig. 2. In order to analyse the radicles as they grew in the opaque substrate without any disturbance, the whole SHs were imaged by means of X-ray micro-CT (see Fig. 2a). All SHs from ISS, GRE and CL experiments were scanned by a Skyscan 1272 desktop microtomograph (Bruker, US) without dismantling them, at 50 kV voltage and 200 μA current. The obtained X-ray projections were subjected to a Feldcamp back-projection procedure in order to obtain the cross-section reconstruction (Fig. 2b) using NRecon software v.1.8 (Bruker, US). 8-bit grey level cross-section images of the SHs were obtained at a resolution of 17 μm (Fig. 2c). Images were all calibrated using the known size of the SH as reference. Further details about acquisition and 3D image reconstruction parameters are reported in Izzo et al. [16]. The images of the radicles were then segmented from the surrounding substrate in the SHs by applying first Otsu threshold method [27] on grey level histograms for the image binarization (Fig. 2d), then the opening mathematical morphology operator with 1 voxel radius (Fig. 2e) and, finally, removing isolated groups of white voxels (despeckle) smaller than eighty voxels (Fig. 2f). Above procedure allowed to remove the substrate from images without shifting the root boundaries except for small protruding parts narrower three voxels

After image processing, an approach based on the recent method of Straumit et al. (2015) was used for the characterization of root local orientation. It is based on the structure tensor concept widely used in image processing in order to describe the distribution of the gradient in a specified neighbourhood around a voxel [29] and was specifically developed to determine local anisotropy tensors in micro-CT image data. It allows to determine local orientation of grey level objects in 3D space by means of local spherical coordinates (θ, φ) (see Fig. 2g) represented by a grey level 8-bit map. An example of the application of Straumit's method on a radicle 3D image is reported in Fig. 3. Such approach is implemented in CTAn software (Bruker, US). It was applied here with a 3D structure matrix 31x31x31 voxels wide and angular resolution of 15° for θ and 30° for φ (see Fig. 3). The polar angle θ was referred to the perpendicular direction to the sowing plane while the azimuthal angle φ lied on a plane parallel to the sowing plane in the SHs (see Fig. 2g and 3). Based on the above settings the two following orientation parameters were defined: (i) the "root angle to sowing plane" (RASP) which is the complementary angle of θ measured locally on the radicles and (ii) the number of "root orientation changes" (ROC) obtained by scoring the changes in θ and φ coordinates observed starting from the seed till the end of a radicle. For RASP, the root volume-based angular distribution was determined.

(See figure on next page.)

Fig. 2 Scheme of root image acquisition, processing and analysis. **a** 3D imaging of carrot radicles from seedlings grown in opaque substrate scanned for the acquisition of the X-ray projections by means of X-ray microtomography. **b** 3D image reconstruction by means of Feldcamp backprojection procedure. **c** Cross-section of the 3D reconstruction. **d** 2D image section and 3D reconstruction resulting from binarization by image thresholding and Volume of interest (VOI) selection (the gray cylinder). **e** 2D image section and 3D reconstruction after opening mathematical morphological operation. **f** 2D image section and 3D reconstruction after despeckle to remove isolated groups of voxels. **g** Local root orientation measurements by spherical coordinates (local zenithal and azimuthal angles θ and φ)

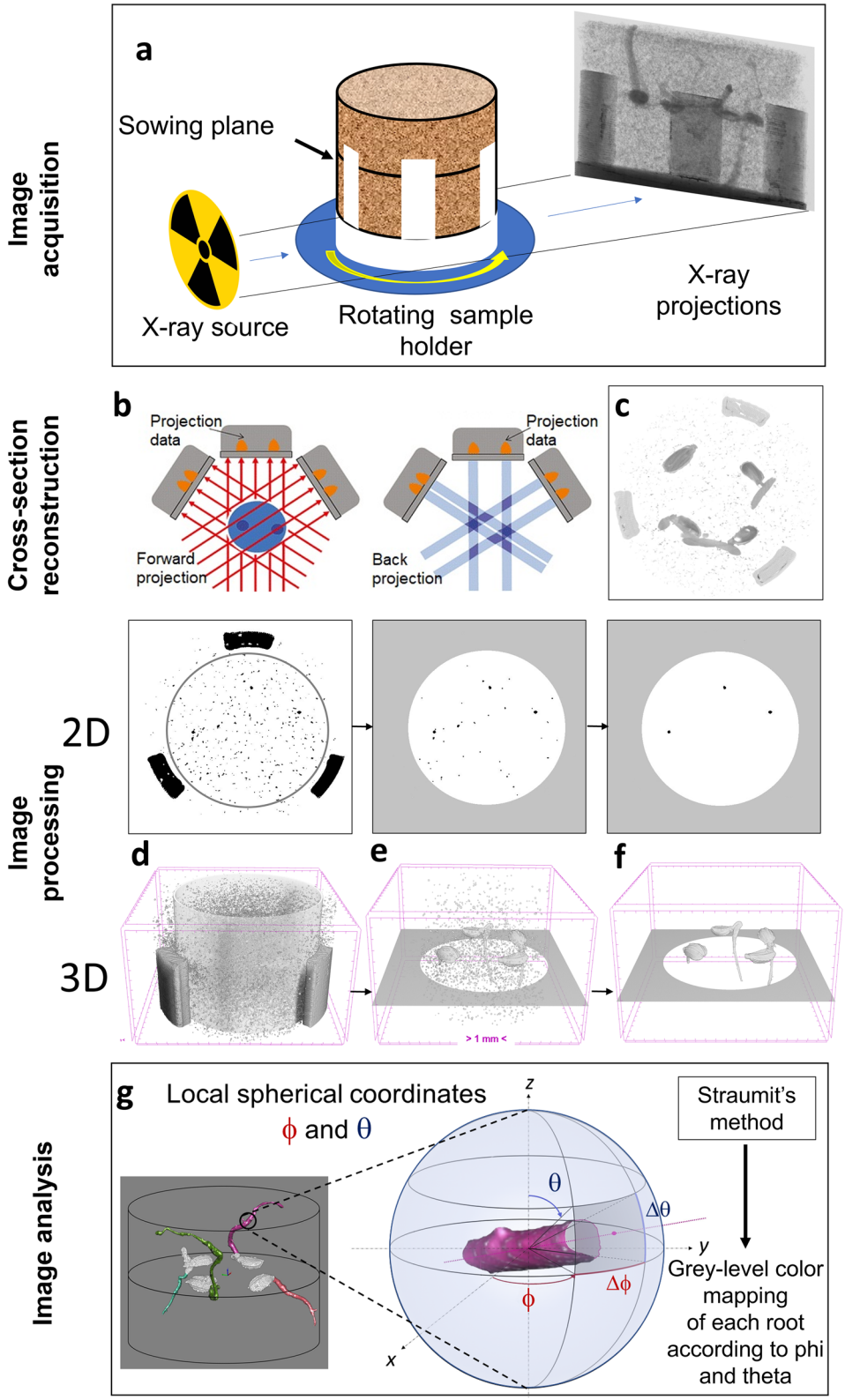

Fig. 2 (See legend on previous page.)

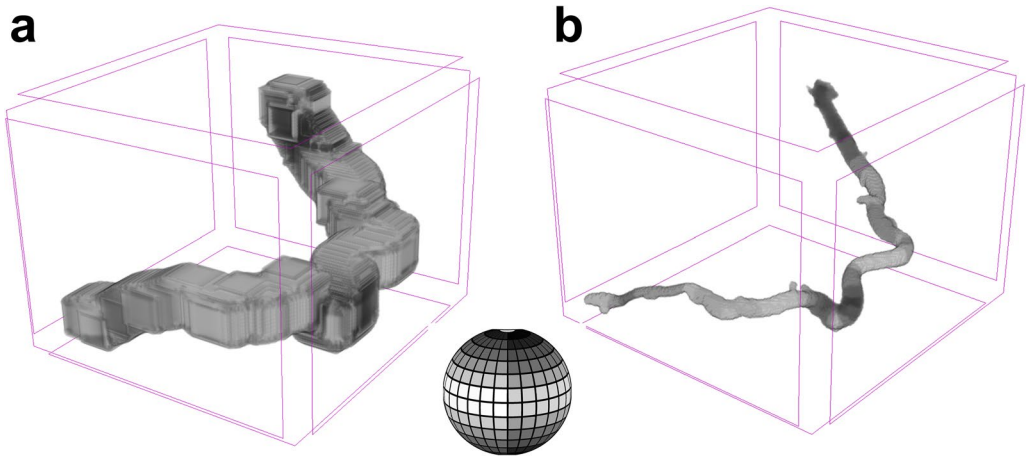

Fig. 3 Local orientation mapping. Example of the application of Straumit's method based on voxel model of structure tensor. **a** 3D gradient matrices of structure tensors calculated around radicle voxels. **b** 3D colour-coded orientation of radicle voxels according to the reported spherical legend

Radicle volume was calculated as the sum of white voxels representing each radicle and the root thickness (RT) distribution was determined by the "successive opening" algorithm (e.g.: [8, 14]) which allows volume-based local thickness definition. After halving the image resolution, the algorithm provides RT classes four times the initial voxel size wide, except for the first class which is six times the voxel size wide. Above image processing and analysis have been performed using CTAn software v.1.20.8 (Bruker, US).

Statistical analysis

One-way ANOVA using the different experiments (ISS, CL and GRE) as factor has been performed on RASP and RT distributions parameters. Then All Pairwise Multiple Comparisons were performed using the Fisher LSD Method. Fisher LSD and Tukey tests were performed on the RASP and RT distribution data, respectively. All statistical tests were performed using the software Sigmaplot 13 (Systat Software Inc.).

Results

The analysed roots in this study were 10 from ISS, 12 from CL and 11 from GRE experiments. A selection of such radicles is shown in the Figs. 4, 6 and 8. All the radicles are shown in the Figures S1, S2 and S3. The approach used for image analysis allowed us to obtain, for each analysed root, the mapping of the portions of root volume characterised by a given orientation with respect to the (i) sowing plane (Fig. 4, Figure S1) and (ii) three-dimensional space (Fig. 6, Figure S2) referred to the SHs used in the experiments (see Fig. 1). In addition, the mapping of the portions of root volume characterised by a given thickness has been obtained (Fig. 8, Figure S3). False colours have been used for the root mapping as reported in the legends of the above figures.

Root angle to sowing plane

In Fig. 4 it can be clearly observed that the roots grown in GRE have obviously a perpendicular orientation to the sowing plane, thus the prevailing colour in these roots is red (corresponding to RASP in the range 75–90°). The roots grown in both simulated and real weightless conditions have sub-parallel orientations to this plane and are characterised by a prevalence of blue and fuchsia root segments (RASP in the range 15–30° and 0–15°).

Regarding the comparison of average RASP distribution parameters between GRE and weightless conditions (CL and ISS), the results in Table 1 indicate that both the mean and modal values are significantly higher in GRE than those in ISS and CL, whereas the opposite happens for the Standard deviation and Skewness index Fisher values. The significantly higher standard deviation of RASP distribution in weightless conditions indicates the greater variability of root orientation obtained in ISS and CL experiments than in GRE. The different sign of Skewness indicates the opposite asymmetry of the RASP distributions in weightless (CL and ISS) vs GRE conditions according to the visual observation of the prevailing subvertical orientation of the roots in GRE. The RASP distribution data and parameters of all the analysed roots are reported in tables S1 and S2.

Figure 5 shows the average RASP distributions of the three experiments with standard error bars and, for each experiment, the results of the statistical pairwise comparison between the angular ranges. The RASP distributions

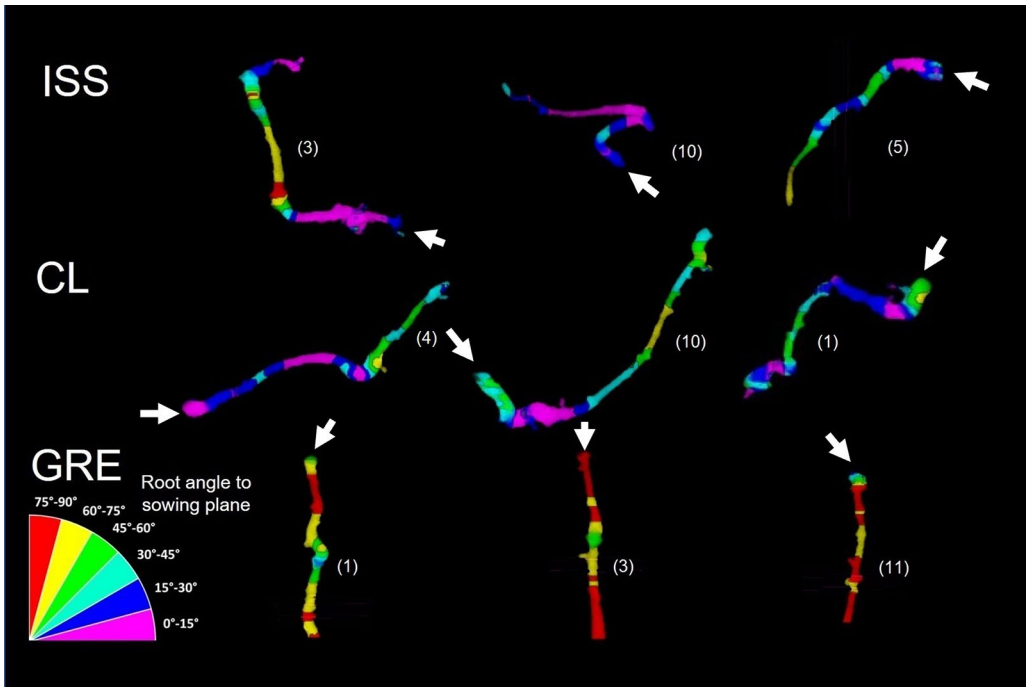

Fig. 4 Root angle to sowing plane mapping. Colour coded images of the parameter "root angle to sowing plane" of three radicles chosen as example for each experiment. The white arrows indicate the root initiation point from seed

Table 1 RASP distribution parameters. Average values of the parameters of the distribution of root angle to sowing plane (RASP) (standard errors in brackets)

	RASP Distribution			
	Mean value (°)	**Modal value (°)**	**Standard dev. (°)**	**Skewness index fisher**
ISS	35.3 (3.8)b	28.6 (8.4)b	21.3 (1.9)a	0.22 (0.28)a
CL	34.5 (3.7)b	33.4 (7.7)b	19.8 (2.1)a	0.50 (0.29)a
GRE	66.4 (2.7)a	73.5 (1.9)a	13.8 (1.2)b	− 0.61 (0.18)b

Values on a column sharing a letter are not statistically different (Fisher LSD test) at $P < 0.05$

a: significantly higher values

b: significantly lower values

of each single root are reported in Figures S4a and S4b. The distributions are evaluated as root volume percentage in 15°-wide angular ranges and were obtained dividing, for each angle range, the sum of the voxels of that angle range by the total of the root voxels. It is possible to observe that the curve trend is very similar for ISS and CL and is, of course, completely different for the GRE in which subvertical angular ranges prevail as provided by the significantly higher root volume percent of the RASP ranges > 60° respect to the others. For ISS and CL, the RASP distribution trends were not significantly different as found considering the statistical results about the distribution parameters reported in Table 1. Such absence of significant difference of RASP between ISS and CL was also confirmed by the Tukey tests of the pairwise comparisons between the angular ranges. Furthermore, the only significant difference in the percent root volume for both ISS and CL is between the angular ranges 0–15° and 76–90°, being the first significantly higher than the second one.

Root orientation changes

Figure 6 shows the colour-coded images of the root orientations in three dimensions considering also the azimuthal angle ϕ. The number of root orientation changes (ROC) was scored along the root length when Δθ was at

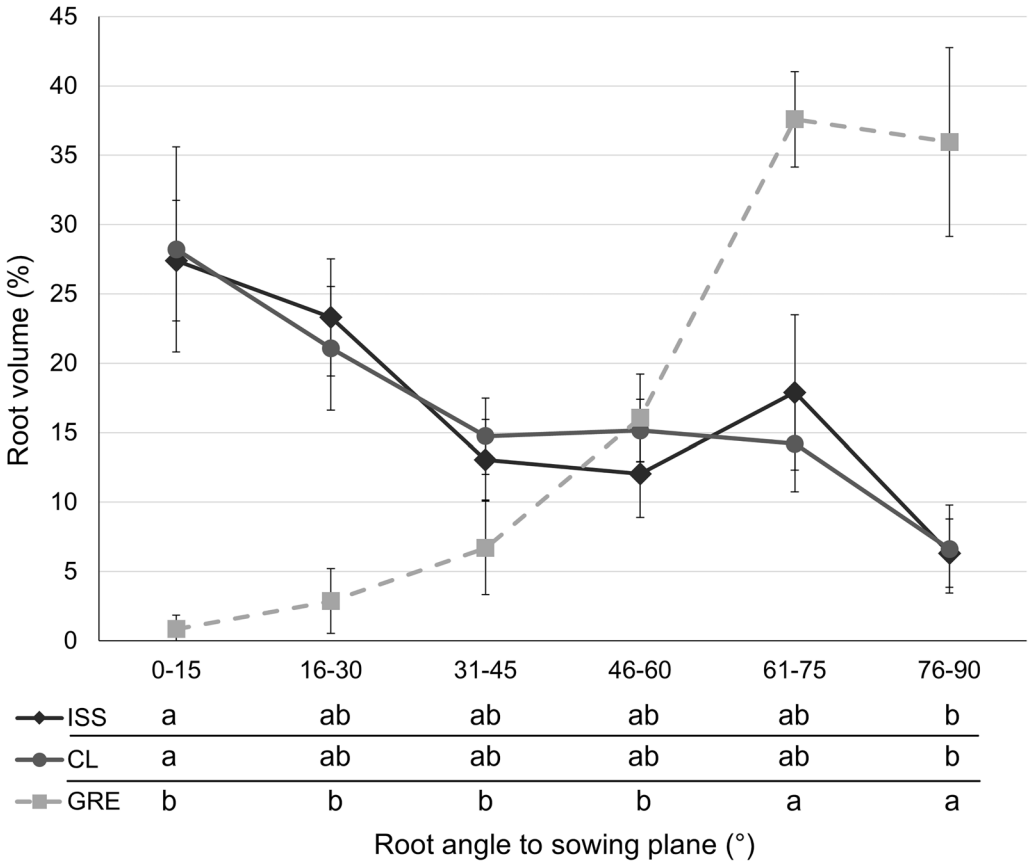

Fig. 5 Root angle to sowing plane (RASP) distribution. Bars are standard errors. Shared letters on a row mean absence of significant (Tukey tests, at a $P < 0.05$) difference of root volume percent among angular ranges

least 30° and Δ∅ at least 120°. Thus, the portions of the root characterised by a given combination of the range of values of the θ and ϕ angles have been represented with 9 different colours, as can be seen from the legend in Fig. 6.

Average values of the number of ROC were then obtained for each experiment and are reported in Fig. 7. ROC numbers of all the analysed roots are reported in table S3.

From Fig. 7 it can be observed that the number of ROC is significantly greater in roots grown on ISS and CL than in roots grown in GRE, as expected.

Root thickness

Figure 8 and Figure S3 show that in all experiments a local thickening of the radicles is observed where a marked orientation change occurs, which sometimes results in a thickness class change.

From the Table 2 it can be noted that the average values of volume of the roots grown in ISS, CL and GRE were not significantly different from each other. Regarding the RT distribution parameters, also the modal value and the standard deviation are not significantly different among the three experiments. Only the mean thickness of CL and the skewness of both ISS and CL resulted significantly different from those of GRE. The RT distribution data and parameters of all the analysed roots are reported in tables S4 and S5.

Regarding the RT distributions, Fig. 9 shows the average values of root volume in each thickness range about 70 µm-wide and the corresponding standard errors bars. The RT distributions of each single root are reported in Figures S5a and S5b. It is possible to observe a higher volume of thinner root portions in ISS and CL than GRE with significant differences up to 306 µm, while significantly higher average volume of 442–510 µm roots is observed for GRE compared to ISS. In such thickness range, CL exhibits a significantly higher average volume than ISS.

Discussion

In this work the study of root growth orientation in weightless conditions has been addressed by using three-dimensional image analysis obtained from micro-CT scans. The X-ray micro-CT imaging of the whole

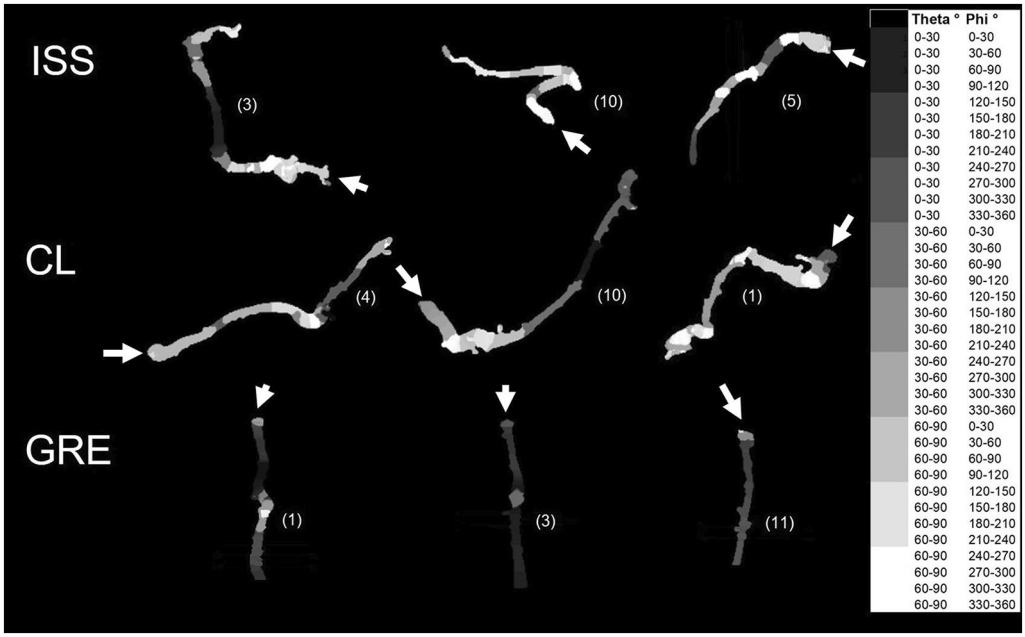

Fig. 6 Root 3D orientation mapping. Colour coded images of three-dimensional orientation measured using spherical coordinates of three radicles chosen as example for each experiment. Each colour corresponds to a combination of values of the spherical coordinates (local zenithal and azimuthal angles θ and φ). The white arrows indicate the root initiation point from seed

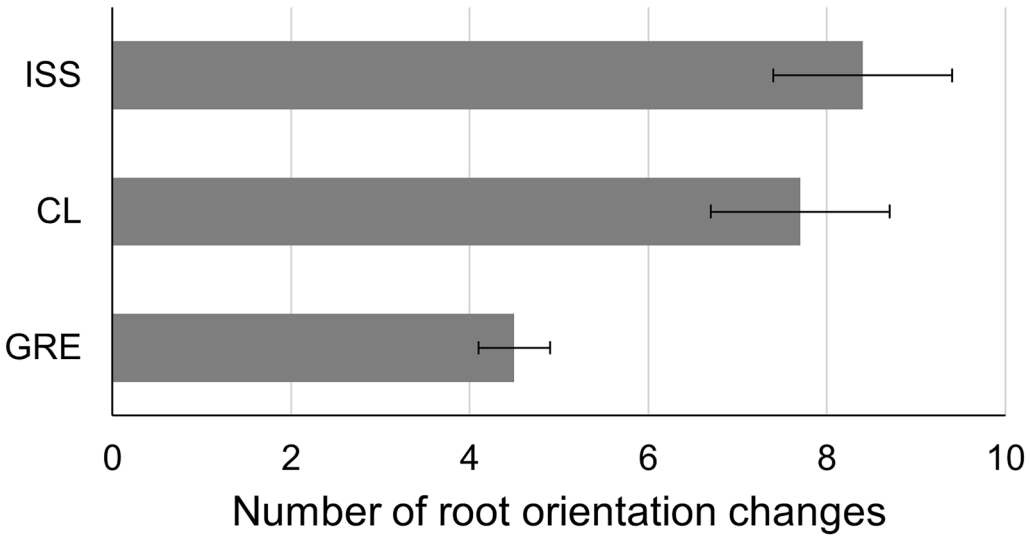

Fig. 7 Root orientation changes (ROC). Average values of the number of ROC. (bars are standard errors). Values sharing a letter are not statistically different (Fisher LSD test) at a $P < 0.05$

substrate holder was chosen as the only option suitable to characterize the root growth in our experimental conditions due to the small size of the hardware available for the project on the ISS. Magnetic resonance imaging (MRI) and positron emission tomography (PET) could be considered alternatives in principle to the X-ray micro-CT. However, high image resolution was required to describe and analyse the small carrot radicles, which is not provided by MRI [24] or PET [25]. In particular this latter technique would have implied the use of a radioactive tracer, which was infeasible on the ISS for safety and decay issues.

On the other hand, manual measurements directly on the roots neither could be done, as after some preliminary

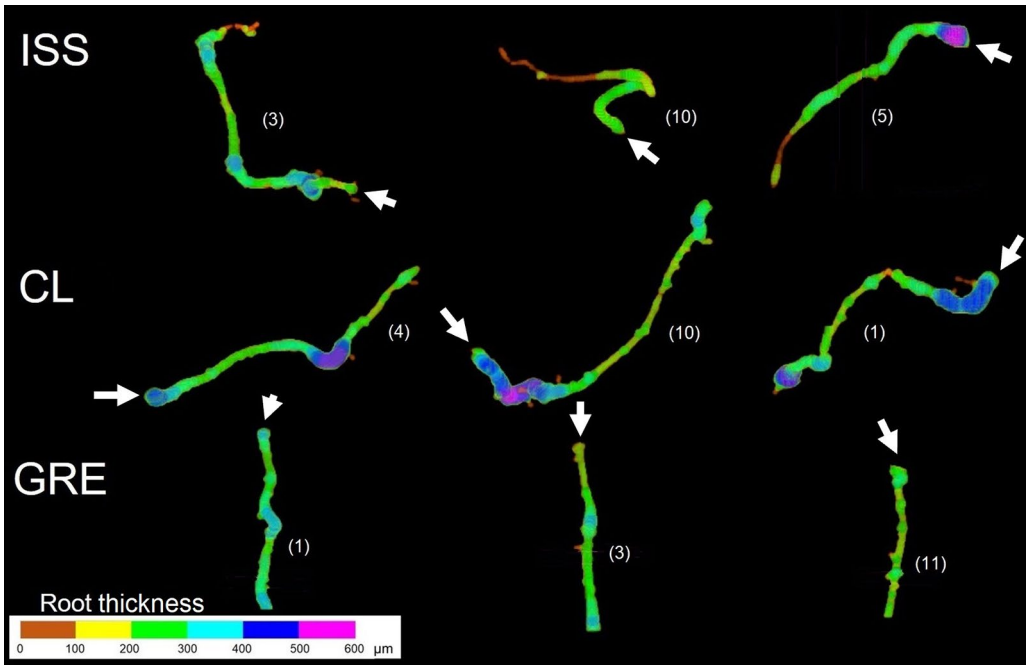

Fig. 8 Root thickness mapping. Colour coded images of the root thickness of three radicles chosen as example for each experiment. The white arrows indicate the root initiation point from seed

Table 2 Root thickness (RT) distribution parameters. Average values of root volumes and parameters of the RT distribution (standard errors in brackets)

	Root volume	Root thickness distribution			
	(mm^3)	Mean value (µm)	Modal value (µm)	Standard deviation (µm)	Skewness index Fisher
ISS	0.66 (0.07)a	316.0 (19.9)ab	326.4 (30.1)a	87.9 (7.5)a	− 0.22 (0.13)a
CL	0.69 (0.12)a	295.8 (26.6)b	311.7 (39.7)a	85.5 (8.5)a	− 0.19 (0.10)a
GRE	0.63 (0.09)a	363.4 (18.6)a	364.7 (26.4)a	74.1 (5.1)a	− 0.72 (0.22)b

Values on a column sharing a letter are not statistically different (Fisher LSD test) at $P < 0.05$

a: significantly higher values

b: significantly lower values

tests trying to disassemble Oasis disks where carrot radicles grew, these latter broke or lost their geometry.

The used method of local orientation characterization has been very recently developed to detect anisotropies in generic micro-CT images and has been applied here to characterise the root orientation. Other X-ray CT-based studies on 3D root architecture (e.g., [9, 31, 35, 36]) characterised root orientation as a whole by measuring the direction of a specific couple of points on the roots. Conversely, the Straumit's approach [34] used here allows to quantify locally the orientation of root portions by tuning both root portion minimal length and angular resolution as needed. To be aware that the proposed image analysis approach is a mathematical morphology one and thus requires stacks of raster images of roots. Therefore, it cannot be directly applied if the root imaging method provides 3D vector graphic models of the roots. In such a case, images have to be first converted in raster mode. A limit of the Straumit's approach is that it was designed to work on 8-bit images and therefore to encode in theory no more than 256 grey levels. This means that actually a discrete number of 3D root orientations not exceeding 256 could be identified. In practice, aiming at obtaining a homogeneous step of discretization in all possible directions (phi and theta), the number of discrete orientations identifiable by means of the method has been 144. Such limitation could be overcome in the future by implementing

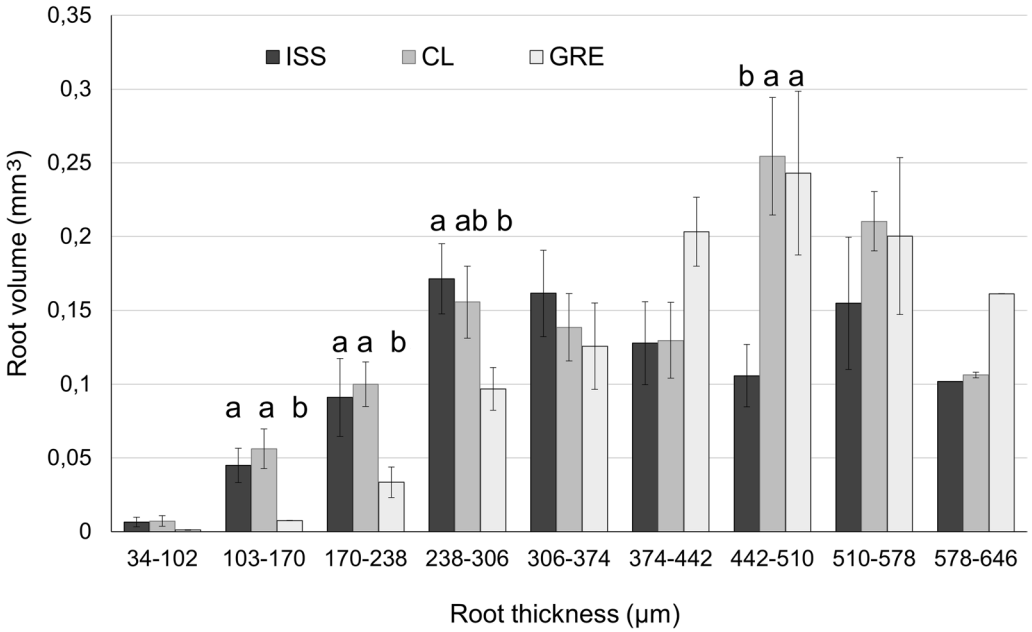

Fig. 9 Root thickness (RT) distributions. Average values of root volume for each root thickness class (bars are standard errors). Values sharing a letter are not statistically different (Fisher LSD test) at a $P < 0.05$

a method similar to that of Straumit, but applicable to images with more than 8 bits (e.g., 16 bits). Nevertheless, in our study the discretisation of the theoretically infinite 3D orientations to 144 has not been a real limitation. Indeed, small random changes in radicle orientation can be physiological while we were interested to marked changes in radicle orientation surely caused by the abiotic stress of weightlessness. The use of such approach allowed to map the local orientation of carrot radicles grown in ISS, CL and GRE experiments, even if it has the potential to be applied to larger and more complex root systems. In fact, the proposed local orientation mapping appr

oach is independent from the size of the analysed root system and, without the hardware size limitation we faced with the experiment on the ISS, it could be applied to larger root systems imaged using for example medical CT scanners larger than X-ray micro-CT. In addition, a simple root system like that of carrot seedlings studied here can be regarded as an elementary component of a complex root system. On the other hand, as demonstrated by Rangarajan and Lynch [28] by means of in silico simulations, phenotyping of complex root architectures must be carried out at their elementary level of organization to get a better understanding of the interactions among single traits and to identify their genetic features (QTLs). Moreover, it is possible to define other orientation parameters than RASP and ROC starting from the same kind of orientation maps, depending on the specific architecture of the analysed root system and according to the specific aims of the study.

The specific goal of this study was to compare the root growth orientation in the real vs simulated weightlessness experiments using the proposed approach. The GRE experiment has been added to assess the sensitivity of the used local orientation parameters and as a test for the image analysis method with radicles having the *a priori* known overall vertical orientation. Two new root orientation traits, the "root angle to sowing plane" (RASP) and the "root orientation changes" (ROC) were defined, in addition of measuring the root thickness (RT) to thoroughly analyse the root growth of the carrot seedlings. The RASP is a local parameter whereas the ROC refers to the whole radicle although it is, as well, based on the three-dimensional local orientation scored on the roots. For the RASP the angular distribution in root volume percent was determined, whereas for RT the distribution in absolute root volume. The found distributions of RASP and RT were then analysed in terms of both comparison of distribution parameters and class by class.

Notwithstanding the very accurate comparison, any significant difference in orientation of carrot roots grown in ISS and CL was not found. In particular, a common root orientation characteristic found in both ISS and CL experiments was the absence of a prevailing orientation (RASP) except for the significant volumetric prevalence of subparallel (0–15° oriented) root portions respect to

sub-orthogonal (76–90°oriented) ones to the sowing plane. This could be favoured by the fact that the sowing plane represents a discontinuity between the two semi-substrates constituting the SHs and therefore it determines a lower mechanical impedance to the root development. Furthermore, the ROC results showed that in both weightless conditions (simulated and real) the number of changes in root orientation is almost doubled compared to GRE.

Also, the volume of all radicles in ISS and CL did not show any significant difference, indicating the same developmental stage for all the studied seedlings. Actually, the only significant difference which was found comparing the overall growth of carrot roots between ISS and CL experiments was in RT distribution and it was detected only after class-by-class analysis. Indeed, a significant volumetric prevalence of the 442–510 µm thickness range was found in the radicles of CL experiment respect to those of ISS, as only difference. It is noteworthy that such thickness range was often found in correspondence of the marked local changes observed in the root orientation (see Fig. 8 and Figure S3), thus the only morphological difference between carrot radicles grown in simulated vs real weightlessness seems to be a larger swelling in the root corners in CL than ISS.

Overall, such findings allowed to give an experimental demonstration of the effectiveness of the clinorotation approach to simulate weightlessness in radicle growth. Thus, the root growth during the seedling development under uniaxial clinorotation can be considered one of the cases in which the great differences often observed in plant growth between weightlessness analogs and weightless spaceflights (e.g., [21, 22]) do not occur. The proper experimental setup used in this study surely contributed to obtaining such results. In fact, it fulfilled all the conditions of using (i) seed stock, (ii) growth substrate, (iii) nutrient media, (iv) temperature and also (v) containers identical to those of spaceflight experiment as suggested by Kiss [19] in order to maximise the comparability of outcomes from simulated weightlessness and spaceflight experiments.

Conclusions

In this work a recent 3D image analysis approach was proposed to accurately characterise the phenotypic trait of plant root orientation, mapped locally along carrot radicles imaged by X-ray micro-CT, grown in real and simulated weightless conditions.

Simulated weightless conditions by means of clinorotation provided a very similar radicle development compared to radicles grown on the ISS, indicating that the used weightlessness analog can be a reliable and affordable tool to address plant physiology studies which require an experimental design with alteration of gravity.

Notwithstanding the very specific root system and purposes of this study case, the proposed local orientation mapping method can be extended also to different root systems thus providing a contribution in the challenging task of phenotyping complex and important plant structures such as roots.

Supplementary Information

The online version contains supplementary material available at https://doi.org/10.1186/s13007-024-01276-2.

Additional file 1: Figure S1. Root angle to sowing plane mapping. Colour coded images of the root angle to sowing plane of all the radicles for each experiment

Additional file 2: Figure S2. Root orientation changes mapping. Colour coded images of the number of root orientation changes of all radicles for each experiment

Additional file 3: Figure S3. Root thickness mapping. Colour coded images of the root thickness of all radicles for each experiment

Additional file 4: Figure S4a. Root angle to sowing plane distributions. Numbers are root IDs

Additional file 5: Figure S4b. Root angle to sowing plane distributions. Numbers are root IDs

Additional file 6: Figure S5a. Root thickness distributions. Numbers are root IDs

Additional file 7: Figure S5b. Root thickness distributions. Numbers are root IDs

Additional file 8

Acknowledgements
Not applicable.

Author contributions
G.M. conceived the idea of the methodological approach, did X-ray micro-CT scans and image processing. L.G.I., L.E.R. and G.A. performed the root growth experiments. L.G. did 3D image analysis. L.G. and G.M.prepared the manuscript and interpreted and discussed results. G.A. was the responsible of the funding project. G.M., L.G., L.G.I., G.A. contributed to critical revision of the text.

Funding
This research has been financially supported by the agreement between Italian Space Agency (ASI) and the University of Naples Federico II (MULTITROP, n. 2017-016-H.0). ASI coordinated the program and provided the access to the ISS and to the onboard resources thanks to the Memorandum of Understanding between ASI and NASA for the design, development, operation, and utilization of three mini pressurized logistic modules for the ISS.

Availability of data and materials
No datasets were generated or analysed during the current study.

Declarations

Ethics approval and consent to participate
Not applicable.

Consent for publication
Not applicable.

Competing interests
The authors declare no competing interests.

Received: 24 July 2024 Accepted: 23 September 2024
Published online: 28 September 2024

References

1. Aronne G, Muthert LWF, Izzo LG, Romano LE, Iovane M, Capozzi F, Manzano A, Ciska M, Herranz R, Medina FJ, Kiss JZ, van Loon JJWA. A novel device to study altered gravity and light interactions in seedling tropisms. Life Sci Space Res. 2022;32:8–16. https://doi.org/10.1016/j.lssr.2021.09.005.
2. Aronne G, Romano LE, Izzo LG. Subsequent inclusion/exclusion criteria to select the best species for an experiment performed on the ISS in a refurbished hardware. Life Sci Space Res. 2020;27:19–26. https://doi.org/10.1016/j.lssr.2020.07.002.
3. Bartsev SI, Gitelson JI, Lisovsky GM, Mezhevikin VV, Okhonin VA. Perspectives of different type biological life support systems (BLSS) usage in space missions. Acta Astronaut. 1996;39(8):617–22. https://doi.org/10.1016/S0094-5765(97)00012-X.
4. Cowles JR, Scheld HW, Peterson C, LeMay R. Growth and development of plants flown on the STS-3 space shuttle mission. Acta Astronaut. 1984;11(5):275–7. https://doi.org/10.1016/0094-5765(84)90011-0.
5. De Micco V, De Pascale S, Paradiso R, Aronne G. Microgravity effects on different stages of higher plant life cycle and completion of the seed-to-seed cycle. Plant Biol. 2014;16:31–8. https://doi.org/10.1111/plb.12098.
6. De Micco V, Aronne G, Colla G, Fortezza R, De Pascale S. Agro-biology for bioregenerative life support systems in long-term space missions: general constraints and the Italian efforts. J Plant Interact. 2009;4(4):241–52. https://doi.org/10.1080/17429140903161348.
7. De Pascale S, Arena C, Aronne G, De Micco V, Pannico A, Paradiso R, Rouphael Y. Biology and crop production in Space environments: challenges and opportunities. Life Sci Space Res. 2021;29:30–7. https://doi.org/10.1016/j.lssr.2021.02.005.
8. Dougherty ER, Lotufo RA, Bellingham WA. Hands-on morphological image processing. Bellingham: SPIE Press; 2003. https://doi.org/10.1117/3.501104.
9. Flavel RJ, Guppy CN, Tighe MK, Watt M, Young IM. Quantifying the response of wheat (Triticum aestivum L) root system architecture to phosphorus in an Oxisol. Plant Soil. 2014;385(1):303–10. https://doi.org/10.1007/s11104-014-2191-9.
10. Gerth S, Claußen J, Eggert A, Wörlein N, Waininger M, Wittenberg T, Uhlmann N. Semiautomated 3D root segmentation and evaluation based on X-ray CT imagery. Plant Phenomics. 2021. https://doi.org/10.34133/2021/8747930.
11. Hargreaves CE, Gregory PJ, Bengough AG. Measuring root traits in barley (Hordeum vulgare ssp. vulgare and ssp. spontaneum) seedlings using gel chambers, soil sacs and X-ray microtomography. Plant Soil. 2009;316:285–97. https://doi.org/10.1007/s11104-008-9780-4.
12. Hasenstein KH, Van Loon JJWA, Beysens D. Clinostats and other rotating systems—design, function, and limitations. Generat Appl Extra-Terrestrial Environ Earth. 2015;14:147–56.
13. Herrero-Huerta M, Meline V, Iyer-Pascuzzi AS, Souza AM, Tuinstra MR, Yang Y. 4D Structural root architecture modeling from digital twins by X-ray computed tomography. Plant Methods. 2021;17(1):1–12. https://doi.org/10.1186/s13007-021-00819-1.
14. Hildebrand T, Rüegsegger P. A new method for the model-independent assessment of thickness in three-dimensional images. J Microsc. 1997;185:67–75. https://doi.org/10.1046/j.1365-2818.1997.1340694.x.
15. Hoson T. Automorphogenesis of maize roots under simulated microgravity conditions. Plant Soil. 1994;165(2):309–14. https://doi.org/10.1007/BF00008074.
16. Izzo LG, Romano LE, De Pascale S, Mele G, Gargiulo L, Aronne G. Chemotropic vs hydrotropic stimuli for root growth orientation in microgravity. Front Plant Sci. 2019. https://doi.org/10.3389/fpls.2019.01547.
17. Izzo LG, Romano LE, Muthert LWF, Iovane M, Capozzi F, Manzano A, Ciska M, Herranz R, Medina FJ, Kiss JZ, van Loon JJWA, Aronne G. Interaction of gravitropism and phototropism in roots of Brassica oleracea. Environ Exp Bot. 2022;193: 104700. https://doi.org/10.1016/j.envexpbot.2021.104700.
18. Kato Y, Abe J, Kamoshita A, Soil JY-P. Genotypic variation in root growth angle in rice (Oryza sativa L) and its association with deep root development in upland fields with different water regimes. Plant Soil. 2006;287(1–2):117–29. https://doi.org/10.1007/s11104-006-9008-4.
19. Kiss JZ. Conducting plant experiments in space. Meth Molec Biol. 2015;1309:255–83. https://doi.org/10.1007/978-1-4939-2697-8_19.
20. Kiss JZ, Katembe WJ, Edelmann RE. Gravitropism and development of wild-type and starch-deficient mutants of Arabidopsis during spaceflight. Physiol Plant. 1998;102(4):493–502. https://doi.org/10.1034/j.1399-3054.1998.1020403.x.
21. Kiss JZ, Wolverton C, Wyatt SE, Hasenstein KH, van Loon JJ. Comparison of microgravity analogs to spaceflight in studies of plant growth and development. Front Plant Sci. 2019;10:1577. https://doi.org/10.3389/fpls.2019.01577.
22. Kozeko LY, Buy DD, Pirko YV, Blume YB, Kordyum EL. Clinorotation affects induction of the heat shock response in Arabidopsis thaliana seedlings. Gravit Space Res. 2018;6:2–9. https://doi.org/10.2478/gsr-2018-0001.
23. Medina FJ, Herranz R, Arena C, Aronne G, De Micco V. Growing plants under generated extra-terrestrial environments: Effects of altered gravity and radiation. In: Beysens D, Van Loon JJWA, editors. Generation and applications of extra-terrestrial environments on earth. New York: River Publishers; 2015. p. 239–54.
24. Metzner R, Eggert A, van Dusschoten D, Pflugfelder D, Gerth S, Schurr U, Uhlmann N, Jahnke S. Direct comparison of MRI and X-ray CT technologies for 3D imaging of root systems in soil: potential and challenges for root trait quantification. Plant Methods. 2015;11:1–11.
25. Miyoshi Y, Nagao Y, Yamaguchi M, Suzui N, Yin YG, Kawachi N, Yoshida E, Takyu S, Tashima H, Yamaya T. Plant root PET: visualization of photosynthate translocation to roots in rice plant. J Instrum. 2021;16(12):C12018.
26. Oluwafemi FA, Ibraheem O, Fatoki TH. Clinostat microgravity impact on root morphology of selected nutritional and economic crops. Plant Cell Biotechnol Mol Biol. 2020;21(43&44):92–104.
27. Otsu N. A threshold selection method from gray-level histograms. IEEE Trans Sys Man Cyber. 1979;9(1):62–6. https://doi.org/10.1109/TSMC.1979.4310076.S2CID15326934.
28. Rangarajan H, Lynch JP. A comparative analysis of quantitative metrics of root architecture. Plant Phenomics. 2021. https://doi.org/10.34133/2021/6953197.
29. Rao AR, Schunck BG. Computing oriented texture fields. Cvgip-Graph Models Image Process. 1991;53(2):157–85.
30. Romano LE, Aronne G. The world smallest plants (Wolffia Sp) as potential species for bioregenerative life support systems in space. Plants. 2021;10(9):1896. https://doi.org/10.3390/plants10091896.
31. Schmitz R, Atkinson BS, Sturrock CJ, Hausmann L, Toepfer R, Herzog K. High-resolution 3D phenotyping of the grapevine root system using X-ray Computed Tomography. Vitis. 2021;60(1):21–7. https://doi.org/10.5073/vitis.2021.60.21-27.
32. Shao MR, Jiang N, Li M, Howard A, Lehner K, Mullen JL, Gunn SL, McKay JK, Topp CN. Complementary phenotyping of maize root system architecture by root pulling force and X-ray imaging. Plant Phenomics. 2021. https://doi.org/10.34133/2021/9859254.
33. Singh V, van Oosterom EJ, Jordan DR, Hunt CH, Hammer GL. Genetic variability and control of nodal root angle in sorghum. Crop Sci. 2011;51(5):2011–20. https://doi.org/10.2135/CROPSCI2011.01.0038.
34. Straumit I, Lomov SV, Wevers M. Quantification of the internal structure and automatic generation of voxel models of textile composites from X-ray computed tomography data. Compos A Appl Sci Manuf. 2015;1(69):150–8. https://doi.org/10.1016/j.compositesa.2014.11.016.
35. Teramoto S, Tanabata T, Uga Y. RSAtrace3D: robust vectorization software for measuring monocot root system architecture. BMC Plant Biol. 2021;21(1):1–11. https://doi.org/10.1186/s12870-021-03161-9.
36. Tracy SR, Black CR, Roberts JA, Sturrock C, Mairhofer S, Craigon J, Mooney SJ. Quantifying the impact of soil compaction on root system architecture in tomato (Solanum lycopersicum) by X-ray micro-computed tomography. Ann Bot. 2012;110(2):511–9. https://doi.org/10.1093/aob/mcs031.
37. Villacampa A, Fañanás-Pueyo I, Medina FJ, Ciska M. Root growth direction in simulated microgravity is modulated by a light avoidance mechanism mediated by flavonols. Physiol Plantarum. 2022. https://doi.org/10.1111/ppl.13722.

38. Villacampa A, Sora L, Herranz R, Medina FJ, Ciska M. Analysis of gravireSponse and biological effects of vertical and horizontal clinorotation in Arabidopsis thaliana root tip. Plants. 2021;10(4):734. https://doi.org/10.3390/plants10040734.
39. Wulfsohn D, Nyengaard JR. Simple stereological procedure to estimate the number and dimensions of root hairs. Plant Soil. 1999;209:129–36. https://doi.org/10.1023/A:1004500830178.
40. Wulfsohn D, Nyengaard JR, Gundersen HJG, Cutler AJ, Squires TM. Nondestructive, stereological estimation of plant root lengths, branching pattern and diameter distribution. Plant Soil. 1999;214:15–26. https://doi.org/10.1023/A:1004642820669.
41. York LM, Slack S, Bennett MJ, Foulkes J. Wheat shovelomics II: revealing relationships between root crown traits and crop growth. bioRxiv. 2018;44(March):1–22. https://doi.org/10.1101/280917.

Publisher's Note